

Stretched extra dimensions and bubbles of nothing in a toy model landscape.

I-Sheng Yang*

*ISCAP and Physics Department
Columbia University, New York, NY, 10027, U.S.A.*

Using simple 6D junction conditions, we describe two surprising geometries. First in a case of transitions between $dS_4 \times S_2$ vacua, the S_2 can be stretched significantly larger than the vacuum values both before and after the transition. Then we discover that the naïve instability to decompactification is actually a bubble of nothing instead.

I. INTRODUCTION AND OUTLINE

The six dimensional Einstein-Maxwell theory[1, 2] provides stable compactifications to $M_4 \times S_2$, where M_4 can be deSitter, anti-deSitter or Minkowski space. Recently it is recognized as a good toy model to study transitions between different vacua with compactified extra dimensions[3–5], a scenario that arises from the landscape of string theory[6].

One advantage of this model is that we can have a lot of 4D vacuum solutions with similar sizes of S_2 . Therefore, it is natural to assume that S_2 remains in a similar size during vacuum transitions, as we usually do in more detailed models. However, Johnson and Larfors in[7] pointed out a problem of such assumption in a string theory model.

In Sec.II, we will give an intuitive picture explaining why freezing the extra dimensions during vacuum transitions is generally not a good idea.

In Sec.III, we go over general equations in the 6D Einstein-Maxwell theory. In particular how to describe the vacuum solutions and transitions between them from a purely geometric point of view.

In Sec.IV, we study 4D to 4D transitions with the geometric method and the conventional dimensional reduced method side by side. Together they allow us to describe how the extra dimension changes during the transition. Choosing some allowed values of a free parameter ensures that the extra dimensions are stretched during the process.

In Sec.V, we use the same construction for a new 4D to 6D transition. Different from both the compactification[5] and the decompactification[8], our solution does not have 6D asymptotics. It is similar to a bubble of nothing[9] within a 4D vacuum.

Finally, in Sec.VI we summarize and comment on possible future directions. The stretched extra dimensions may change our picture on bubble collisions[4, 10], and help to clarify whether in some cases the transition will be forbidden[7]. The bubble of nothing [9] may replace the decompactification to be the universal instability in models with extra dimensions.

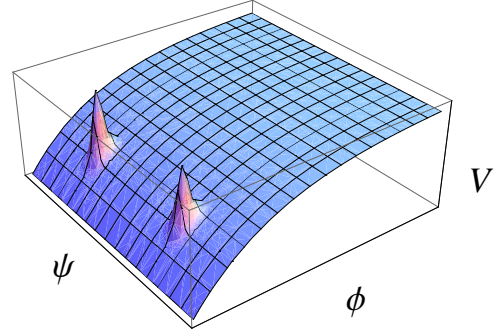


FIG. 1. An effective Euclidean potential for a theory with extra dimensions and discrete vacua. ϕ is related to the size of extra dimension, so there is a decompactification direction where V is asymptotically zero. In 2 different values of ψ but very similar values of ϕ we have two local maxima—the vacua.

II. BETTER NOT TO FREEZE THE EXTRA DIMENSIONS

Fig.1 is a typical effective (Euclidean) potential of a theory with extra dimensions and discrete vacua. It contains the following 2 traits.

- In the ϕ direction, the potential gradually slopes to zero, which corresponds to decompactifying the extra dimensions. This can be the real part of Kähler moduli for string theory[11].
- Discrete vacua distribute not only in the above direction, but also in some other directions ψ . For example the imaginary part of Kähler moduli in[12].

Because the discrete vacua are stabilized by non-perturbative effects, for the value ψ not supporting any vacuum, the effective potential typically follows the general slope in ϕ .

Now consider 2 vacua with the same value of ϕ , namely the same size of extra dimensions. Fixing that size during a transition implies connecting the 2 vacua by a straight line in Fig.1. This line certainly does not obey any equation of motion, as it should be swept away by the non-zero

* E-mail me at: isheng.yang@gmail.com

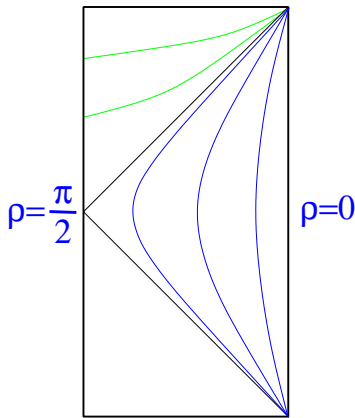


FIG. 2. The special Penrose diagram for dS_6 where two S_2 s are suppressed individually. One of them has zero size on the left boundary, and the other one is zero on the right boundary. Our coordinate covers the region with blue (timelike) slices where the physical radius of one S_2 , $B(\rho)$, is constant, and the radius of dS_3 formed by the other S_2 with time, $A(\rho)$, is also constant. These are the slicings convenient to put the charged brane. The green slices are the similar constant size surfaces with $B > L$, which can be obtained by analytically continuing our coordinate.

slope in the ϕ direction. A more reasonable path representing the transition would be like a projectile motion—climb the slope in ϕ direction and come back, in the meanwhile move from one vacuum to another. This implies the extra dimension during a transition can be very different from its vacuum value.

Such transition might be very annoying to model, since a generic multidimensional effective potential will not be as simple as Fig.1 and one can only search for the path numerically. In the following 2 sections we will show that in the 6D Einstein-Maxwell theory, there is a simple way to monitor transitions with significant changes in the extra dimensions.

III. 6D SPACETIME WITH VACUUM ENERGY AND FLUX

A. Stable solutions

We consider the 6D Einstein-Maxwell theory with positive vacuum energy Λ_6 and 4-form fields, as it is necessary to ensure $dS_4 \times S_2$ compactifications. For the solutions we will use in this paper, it is most convenient to write down a general metric with $SO(3, 1) \times SO(3)$ symmetry.

$$ds^2 = d\rho^2 + A^2(\rho)dS_3^2 + B^2(\rho)d\Omega_2^2. \quad (1)$$

The Einstein equations are

$$\frac{1}{m_6^4} \left(\Lambda_6 + \frac{Q^2}{4B^4} \right) = 3 \frac{1 - \dot{A}^2}{A^2} - 6 \frac{\dot{A}\dot{B}}{AB} + \frac{1 - \dot{B}^2}{B^2}, \quad (2)$$

$$\frac{1}{m_6^4} \left(\Lambda_6 + \frac{Q^2}{4B^4} \right) = \frac{1 - \dot{A}^2}{A^2} - 2 \frac{\ddot{A}}{A} - 4 \frac{\dot{A}\dot{B}}{AB} + \frac{1 - \dot{B}^2}{B^2} - 2 \frac{\ddot{B}}{B},$$

$$\frac{1}{m_6^4} \left(\Lambda_6 - \frac{Q^2}{4B^4} \right) = 3 \frac{1 - \dot{A}^2}{A^2} - 3 \frac{\ddot{A}}{A} - 3 \frac{\dot{A}\dot{B}}{AB} - \frac{\ddot{B}}{B}.$$

Here m_6 is the 6D planck mass and Q is the quantized charge as the field sources, namely 2-branes. The 6D dS space is a solution with $Q = 0$, which corresponds to

$$A(\rho) = L \cos\left(\frac{\rho}{L}\right), \quad (3)$$

$$B(\rho) = L \sin\left(\frac{\rho}{L}\right), \quad (4)$$

where $0 < \rho < \pi/2$, $10m_6^4 L^{-2} = \Lambda_6$. Of course we can interchange A and B , it is still the same solution.

Nonzero Q induces “compactified” solutions as

$$A(\rho) = \frac{\sin(H\rho)}{H}, \quad (5)$$

$$B(\rho) = R. \quad (6)$$

Here it is given in the convenient form for dS spaces, but we can easily take $H \rightarrow 0$ for Minkowski space and imaginary H for AdS spaces. Using the Einstein equations, we can relate the size of the compactified dimensions R and the 4D hubble constant H to both Q and Λ_6 ¹.

$$3H^2 + \frac{1}{R^2} = \frac{1}{m_6^4} \left(\Lambda_6 + \frac{Q^2}{4R^4} \right), \quad (7)$$

$$6H^2 = \frac{1}{m_6^4} \left(\Lambda_6 - \frac{Q^2}{4R^4} \right). \quad (8)$$

B. Transitions between different solutions

From the geometric point of view, vacuum transitions are related to geometries with solutions of different Q s patched together. For example, two different solutions separated by a charged 2-brane at (\bar{A}, \bar{B}) . Note that a boundary in 6D is a 5D object, but 2-branes are only 3D objects. We have to sprinkle the branes in 2 of the dimensions like dust to construct a 5D boundary.

Such patched solutions must obey Israel junction conditions[15] at the boundary.

$$2 \left(\frac{\dot{A}_1 + \dot{A}_2}{\bar{A}} \right) + 2 \left(\frac{\dot{B}_1 + \dot{B}_2}{\bar{B}} \right) = \frac{1}{m_6^4} \left(\frac{\sigma}{4\pi \bar{B}^2} \right), \quad (9)$$

$$3 \left(\frac{\dot{A}_1 + \dot{A}_2}{\bar{A}} \right) + \left(\frac{\dot{B}_1 + \dot{B}_2}{\bar{B}} \right) = 0. \quad (10)$$

¹ Some of the solutions are unstable[13, 14], but the solutions we use in Sec.IV are all stable ones.

It is basically the integrated Einstein equations with a delta-function source. σ is the total tension (energy density in 2D) of the 2-branes we sprinkled on the $4\pi\bar{B}^2$ sphere. Here the convention is that in spacetime region i , the solution is $(A_i(\rho_i), B_i(\rho_i))$ with the small ρ_i region. (namely, if $\dot{A}_i > 0$, it means A_i is increasing while moving toward the boundary.)

Note the positivity constraint on the tension,

$$\frac{\sigma}{4\pi\bar{B}^2 m_6^4} = -4 \left(\frac{\dot{A}_1 + \dot{A}_2}{\bar{A}} \right) > 0. \quad (11)$$

Combining Eq. (10) with Eq. (2), we have

$$6 \frac{\dot{A}_1^2 - \dot{A}_2^2}{\bar{A}^2} = \frac{Q_1^2 - Q_2^2}{4m_6^4 \bar{B}^4}. \quad (12)$$

These tell us an important message. For example, when $Q_1 < Q_2$, we have $\dot{A}_1^2 < \dot{A}_2^2$. So \dot{A}_2 needs to be negative to make the tension positive. More generally, from the side with the larger Q , this boundary always looks like a small bubble (because the bubble radius is shrinking while we approach the boundary from this side).

IV. 4D TO 4D VACUUM TRANSITIONS

A. Geometric point of view

If we limit ourselves to ideal 4D vacua, where $H^{-1} \gg R$, we have

$$\frac{m_6^4}{R^2} = 2\Lambda_6 \left(1 - \frac{9H^2 m_6^4}{2\Lambda_6} \right), \quad (13)$$

$$\frac{Q^2}{m_6^8} = \frac{1}{\Lambda_6} \left(1 + \frac{3H^2 m_6^4}{\Lambda_6} \right). \quad (14)$$

Note that for these vacua, $R \sim (m_6^4/2\Lambda_6)^{1/2}$ cannot change a lot. This gives us a few advantages. First of all, larger H in our 6D point of view really means a larger effective 4-dimensional cosmological constant. Eq. (12) tells us larger Q should be outside, which agrees with the usual tunneling picture that bigger cosmological constant should be outside. There will be geometries with a clean separation of scales,

$$R^{-1} \gg \bar{A}^{-1} \gg H_2 > H_1, \quad (15)$$

which represent standard thin-wall, small bubbles[16] that does not care for the extra dimensions. Within these solutions, we can simplify further calculations with

$$\dot{A}_1 = -\dot{A}_2 = 1 + O(H_i^2 \bar{A}^2). \quad (16)$$

Combine the junction condition Eq. (10) and Eq. (12), we have

$$\frac{\sigma}{4\pi\bar{B}^2 m_6^4} = \frac{m_6^8 \bar{A} (H_2^2 - H_1^2)}{4\Lambda_6^2 \bar{B}^4}. \quad (17)$$

Furthermore, if B does not change a lot during the transition, we have $\bar{B} \sim R_i \sim R = (m_6^4/2\Lambda_6)^{1/2}$. The entire transition can be understood from the 4D point of view. Using the standard dimensional reduction method, we rescale length and planck mass as following,

$$l_{4D} = l_{6D} R m_6, \\ m_4 = \sqrt{4\pi} m_6.$$

Eq. (17) reproduces the naïve junction condition in 4D

$$\sigma_{4D} = \frac{r_c \Delta \Lambda_{4D}}{3} \quad (18)$$

as expected.

B. Effective 4D theory

From the very beginning, we could have followed[4] and use the standard dimensional reduced effective 4D theory.

$$\sqrt{4\pi} m_6 = m_4, \\ m_6 B(\rho) = e^{\frac{\phi(\tau)}{2m_4}}, \\ m_6 A(\rho) B(\rho) = a(\tau), \\ m_6 B(\rho) d\rho = d\tau.$$

This translates the 6D Einstein equations into the general 4D FRW equations and an equation of motion for the field ϕ .

$$\phi'' + 3 \frac{a'}{a} \phi' = \frac{\partial V}{\partial \phi}, \quad (19)$$

$$\left(\frac{a'}{a} \right)^2 = \frac{1}{3m_4^2} \left(\frac{\phi'^2}{2} - V \right) + \frac{1}{a^2}, \quad (20)$$

$$\frac{a''}{a} = -\frac{1}{3m_4^2} \left(\phi'^2 + V \right). \quad (21)$$

Here ' means the derivative to τ and the effective potential

$$V(\phi) = m_4^2 \left(\frac{\Lambda_6}{m_6^4} e^{-\frac{\phi}{m_4}} - m_6^2 e^{-2\frac{\phi}{m_4}} + \frac{Q^2}{4} e^{-3\frac{\phi}{m_4}} \right). \quad (22)$$

In Fig.3 we sketch the shape of effective potentials with different values of Q and indeed found a local minimum as a stable 4D vacuum. Unfortunately, different 4D vacua are present in different effective potentials, but conventional way to describe a transition only applies to two vacua in the same potential.

However, the 6D description provides a simple answer. As depicted in Fig. 4, 5, the field ϕ follows the potential with Q_1 from its vacuum value until the position of the charged brane, $\bar{\phi} = 2m_4 \ln(m_6 \bar{B})$, then jumps to the other potential with Q_2 and proceeds to the other vacuum.

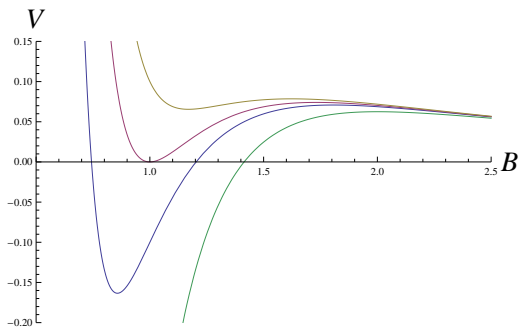


FIG. 3. Effective potential as a function of $B = m_6^{-1} e^{\frac{\phi}{2m_4}}$. From high to low we have potentials with decreasing Q , the stabilized 4D vacuum being deSitter, Minkowski and AdS. The lowest one with $Q = 0$ has no stabilized 4D vacuum.

The velocity ϕ' will be discontinuous at the jump, but can be computed from the extra junction condition in 6D, Eq. (10).

$$\phi'_1 + \phi'_2 = \frac{3\sigma}{\sqrt{4\pi m_6^4 B^3}}. \quad (23)$$

Since ideal 4D vacua are very close together, there will be a range where the following expansion holds in both potentials.

$$V_i(\phi) = \frac{12\pi H_i^2}{R_i^2} + \frac{2\Lambda_6^2}{m_6^{10}} (\phi - \phi_i)^2. \quad (24)$$

Here $e^{\phi_i/2m_4} = m_6 R_i$ is the vacuum value of the field.

We can see the mass of the potential is set by the 6D vacuum energy, which is much larger than the 4D vacuum energy that controls the bounce geometry. By the argument of Coleman, we can ignore the friction term in Eq. (19) and pretend the energy is conserved. Together with the convention we mentioned earlier, that ϕ' is positive if it is increasing toward the brane, we have

$$\phi'_i = \frac{2\Lambda_6}{m_6^5} (\bar{\phi} - \phi_i), \quad (25)$$

where $e^{\bar{\phi}/2m_4} = m_6 \bar{B}$ is the matching value of the field. Plugging into the junction condition Eq. (23), we have

$$\bar{\phi} - \frac{\phi_1 + \phi_2}{2} = \frac{3\sigma m_6}{4\sqrt{4\pi} \bar{B}^3 \Lambda_6}. \quad (26)$$

It is more illuminating to take exponential of the above equation.

$$\frac{\bar{B}^2}{R_1 R_2} = e^{\frac{3\sigma m_6}{4\sqrt{4\pi} m_4 \bar{B}^3 \Lambda_6}}. \quad (27)$$

The matching radius \bar{B} has to be larger than the geometric mean of the vacua radii for the tension to be positive. Also, depending on the tension, the transition

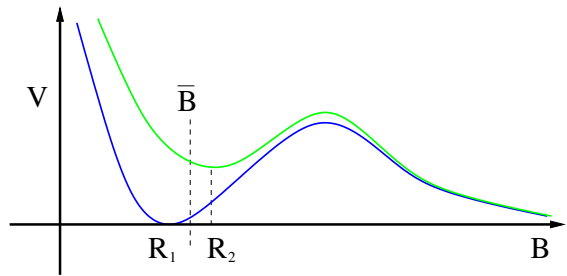


FIG. 4. The effective potential of two solutions with different charges, Q_1 (blue, lower) and Q_2 (green, higher). Our solution corresponds to the radius B started at R_2 , moved through the green (higher) potential to \bar{B} and hit a charged brane, then followed the blue (lower) potential to R_1 .

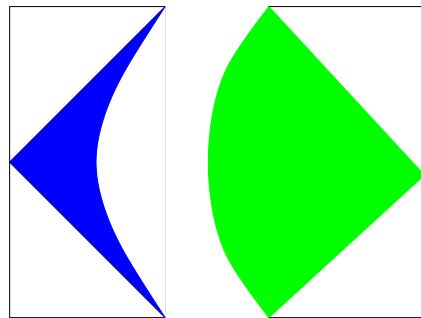


FIG. 5. The corresponding bounce geometry. The charged brane sits on the matching slice of two portions. In the left portion the field ϕ follows the blue potential, and in the right portion it follows the green potential. Our metric describes the shaded parts and can be analytically continued to obtain the rest of the geometry.

can be monotonic as depicted in Fig.4, or with $\bar{B} > R_2$, in which the field goes to a larger value then comes back, as in Fig.6, the extra dimensions are stretched. The critical tension when $\bar{B} = R_2$ is related to the charge ΔQ by Eq. (13),(27) and (14).

$$\sigma_c = 2\sqrt{2\pi} m_6^2 \Delta Q. \quad (28)$$

V. 4D TO 6D SOLUTION

Since the extra dimensions can be stretched during a transition, more dramatic effects like decompactifications might also happen. We can use the same technique of jumping between potentials, but this time from a potential with $Q > 0$ to $Q = 0$. Note that this is not covered in [5] where the entire solution is on one effective potential. The most obvious difference is the charged brane appearing explicitly in our solution.

From Eq. (12) we know that the 4D vacuum has to be outside, since it has the larger Q . It means that the non-trivial region in 4D is only a small bubble, therefore there

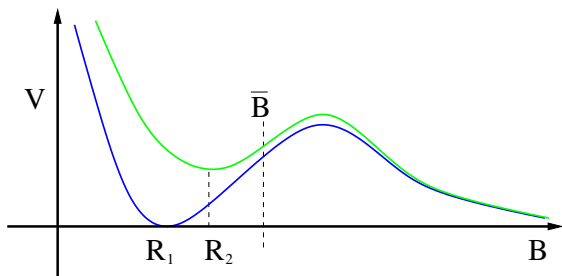


FIG. 6. The matching radius \bar{B} can be larger than either vacuum values R_i .

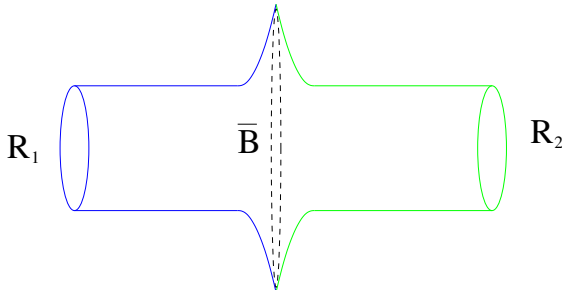


FIG. 7. The size of extra dimension S_2 gets stretched during the transition from vacuum 2 (green, right) to vacuum 1 (blue, left).

is no major difference between a deSitter, Minkowski or AdS space. We shall take the 4D side to be Minkowski space for simplicity. The 6D side has two possibilities. Taking the left portion in Fig.2 we get Fig.8, while the right portion gives Fig.9.

Fig.8 speaks trouble. It contains a piece of deSitter future infinity surrounded by flat spacelike asymptotics. By the argument of Farhi and Guth in [17], it needs to violate the null energy condition. In Appendix A we confirm this by showing explicitly that the junction conditions lead to a domain wall with negative tension.

This leaves us with Fig.9, where the 6D piece is small and does not have deSitter asymptotics. It is just a piece of spacetime letting the extradimensional S_2 pinch off in a non-singular way. In Appendix A we also show by junction conditions that such geometry really exists. Instead of a decompactification, we get a bubble of nothing [9]²!

VI. DISCUSSION

A. Stretched extra dimensions

In Sec.IV B we demonstrated a vacuum transition with extra dimensions stretched, $(\bar{B} - R_i) \gg (R_2 - R_1)$, in

the sense that it seems to get larger than necessary while interpolating between the vacuum values. Within the validity range of our approximations, the sizes of the extra dimensions are still quite similar, $(\bar{B} - R_i) \ll R_i$. It means that we can still understand the geometry in the 4D picture. Also, the stretching process has the time scale of 6D physics, so from the 4D prospective it is very fast, therefore still a thin-wall solution. We did not calculate the tunneling rate explicitly because it will not be significantly different from the pure 4D CDL[16] tunneling.

If we can go beyond the approximation in Eq. (25), we can increase σ even further and describe vacuum transitions with $\bar{B} \gg R_i$. In which case it will be interesting to think about the tunneling rates and many other things. In particular, there might be σ too large that a transition is forbidden as conjectured in[7].

A small stretch described here can already affect one thing—the bubble collisions. An interesting conjecture in[4] says that the domain walls will pass through each other and leave a third vacuum in between, as shown in Fig.10. It is supported by simulations of single-field-tunnelings[10]. The stretches we discovered in this paper unavoidably introduce an additional short-range interaction between domain walls and might change the conclu-

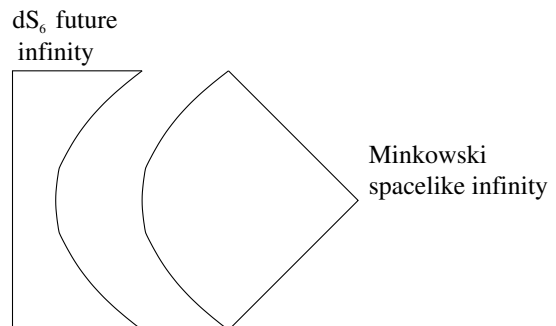


FIG. 8. Matching the interior of a small bubble in 4D Minkowski space to the bigger portion of dS_6 (left hand side of Fig.2). Coexistence of Minkowski spacelike infinity and dS_6 future infinity violates the null energy condition.

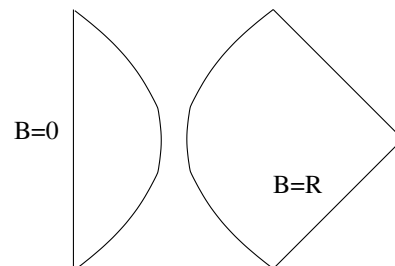


FIG. 9. Matching the interior of a small bubble in 4D Minkowski space to the smaller portion of dS_6 (right hand side of Fig.2). The extra dimension S_2 pinches off smoothly at the left end of this diagram.

² We thank Ben Freivogel for pointing this out.

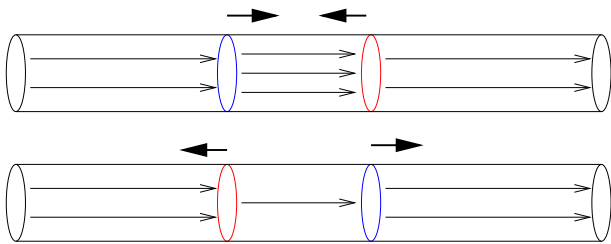


FIG. 10. Bubble collision when the extra dimensions unstretched. The charged branes pass through each other and change the flux in the middle region, generating a third (lower) vacuum. With extra dimensions stretched, the charged branes will not pass through each other this trivially.

sion.

The critical tension to stretch the extra dimensions in Eq. (28) looks very similar to the familiar BPS bound in supersymmetric theories. One may want to argue that for the real string theory landscape, since we started from a supersymmetric theory, the generic object will be much heavier than the bound, therefore always stretches the extra dimensions.

On the other hand, this toy model has 6D vacuum energy to start with. One can also argue that gravity has to be the weakest force[18]³. And there must be a charged brane that does not stretch the extra dimensions.

We will not argue in favor of either side, but simply present this model as a tool to analyze the situation when the extra dimensions are stretched. For the reasons given in the introduction, this might be an unavoidable situation.

B. Bubbles of nothing

In Sec.V and Appendix A we provided two pieces of evidence that a bubble of nothing appears in the place of a decompactification. The Farhi-Guth[17] argument applies to the specific case in Fig.8, where inside the bubble is a deSitter space and outside is flat. We are quite confident that the conclusion still holds when the exterior becomes dS_4 or AdS_4 , because a small bubble effect does not care about asymptotics.

We should think about another case where we cannot apply the Farhi-Guth argument—when the higher dimensional geometry is not deSitter, but flat as in the string theory. It will be very interesting if the junction conditions still work in a similar way as in Appendix A, showing that positive tension demands a bubble of nothing instead of a decompactification.

We need to further study the decay rates. But from the fact that we can arrange our solution to be a small bubble, it should have a rate very similar to a standard thin-wall quantum instanton[4, 16, 19]. Other geometries representing decompactification tunnelings all have rates close to a thermal instanton[4, 5, 8, 11]. This may suggest that bubbles of nothing is the real universal instability we should think about, not decompactifications.

ACKNOWLEDGMENTS

We thank Ben Freivogel for numerous discussions and interesting suggestions that helped to shape this paper. We also thank Raphael Bousso, Matthew Johnson and Robert Myers for stimulating discussions. This work is supported in part by the US Department of Energy, and partially done in the Berkeley Center of Theoretical Physics.

-
- [1] P. G. O. Freund and M. A. Rubin, Phys. Lett. **B97**, 233 (1980).
 - [2] S. Randjbar-Daemi, A. Salam, and J. A. Strathdee, Nucl. Phys. **B214**, 491 (1983).
 - [3] M. R. Douglas and S. Kachru(2006), hep-th/0610102.
 - [4] J. J. Blanco-Pillado, D. Schwartz-Perlov, and A. Vilenkin(2009), arXiv:0904.3106 [hep-th].
 - [5] S. M. Carroll, M. C. Johnson, and L. Randall(2009), arXiv:0904.3115 [hep-th].
 - [6] R. Bousso and J. Polchinski, JHEP **06**, 006 (2000), hep-th/0004134.
 - [7] M. C. Johnson and M. Larfors, Phys. Rev. **D78**, 123513 (2008), arXiv:0809.2604 [hep-th].
 - [8] S. B. Giddings and R. C. Myers, Phys. Rev. **D70**, 046005 (2004), arXiv:hep-th/0404220.
 - [9] E. Witten, Nucl. Phys. **B195**, 481 (1982).
 - [10] R. Easther, J. Giblin, John T., L. Hui, and E. A. Lim(2009), arXiv:0907.3234 [hep-th].
 - [11] S. Kachru, R. Kallosh, A. Linde, and S. P. Trivedi, Phys. Rev. D **68**, 046005 (2003), hep-th/0301240.
 - [12] J. J. Blanco-Pillado *et al.*, JHEP **11**, 063 (2004), arXiv:hep-th/0406230.
 - [13] R. Bousso, O. DeWolfe, and R. C. Myers, Found. Phys. **33**, 297 (2003), hep-th/0205080.
 - [14] C. Krishnan, S. Paban, and M. Zanic, JHEP **05**, 045 (2005), arXiv:hep-th/0503025.
 - [15] W. Israel, Nuovo Cim. **B44S10**, 1 (1966).
 - [16] S. Coleman and F. D. Luccia, Phys. Rev. D **21**, 3305 (1980).
 - [17] E. Farhi and A. H. Guth, Phys. Lett. **B183**, 149 (1987).
 - [18] N. Arkani-Hamed, L. Motl, A. Nicolis, and C. Vafa, JHEP **06**, 060 (2007), hep-th/0601001.
 - [19] A. R. Brown and E. J. Weinberg, Phys. Rev. **D76**, 064003 (2007), arXiv:0706.1573 [hep-th].

³ We thank Robert Myers for pointing this out.

Appendix A: A case study for 4D to 6D transitions

In Sec.IV we followed a general process to find the matching geometry with given Q_1, Q_2, Λ_6 and σ , which relies heavily on the approximation in Eq. (25), and the fact that on either side we can find a family of well-behaved solutions all similar to the 4D stabilized geometry.

Unfortunately, Eq. (25) does not hold anywhere on the $Q = 0$ potential, and even the naive dS_6 solution in Eq. (4) looks dangerously singular in the 4D equations of motion (19). A very careful numerical study might solve the problem, but we would like to do something slightly different here.

Instead of searching for geometries with all parameters fixed, we would like to specify the geometry at the $Q = 0$ side. As a trade off, the tension σ cannot be fixed anymore. We will show that in order to get the geometry in Fig.8, the tension has to be negative. This agrees with our reasoning in Sec.V that it violates the null energy condition. For the geometry in Fig.9, the solution works with a positive tension.

The $Q = 0$ geometry will be specified as the pure dS_6 solution in Eq. 4. With the convention of keeping the small ρ region, it is like Fig.9.

$$\begin{aligned} A_1(\rho) &= L \cos \frac{\rho}{L}, \\ B_1(\rho) &= L \sin \frac{\rho}{L}. \end{aligned} \quad (\text{A1})$$

For Fig.8, we only need to exchange A and B .

$$\begin{aligned} A_1(\rho) &= L \sin \frac{\rho}{L}, \\ B_1(\rho) &= L \cos \frac{\rho}{L}. \end{aligned} \quad (\text{A2})$$

From the junction conditions, Eq. (10), we have

$$\dot{A}_2 = -\frac{\bar{A}\sigma}{16\pi\bar{B}^2m_6^4} - \dot{A}_1, \quad (\text{A3})$$

$$\dot{B}_2 = \frac{3\bar{B}\sigma}{16\pi\bar{B}^2m_6^4} - \dot{B}_1. \quad (\text{A4})$$

By Eq. (14), $Q_2 = m_6^4/\sqrt{\Lambda_6}$ has the 4D Minkowski vacuum. The effective potential is

$$V(\bar{B}) = \frac{2\pi}{R^2\bar{B}^2} \left(1 - \frac{R^2}{\bar{B}^2}\right)^2. \quad (\text{A5})$$

For this potential we can still use the same approximation in Eq. (25).

$$\phi' = \frac{2\sqrt{\pi}}{R\bar{B}} \left(1 - \frac{R^2}{\bar{B}^2}\right). \quad (\text{A6})$$

Relate ϕ' to \dot{B}_2 and use Eq. (A4), we have

$$\dot{B}_1 + \frac{\bar{B}}{2R} \left(1 - \frac{R^2}{\bar{B}^2}\right) = \frac{3\sigma}{16\pi\bar{B}m_6^4}. \quad (\text{A7})$$

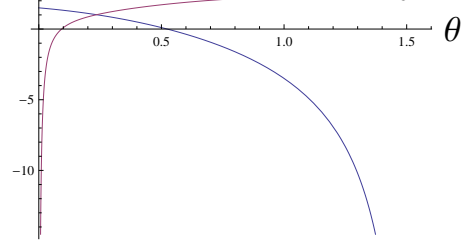


FIG. 11. The two junction conditions for the bubble of nothing geometry. They cross at a positive σ .

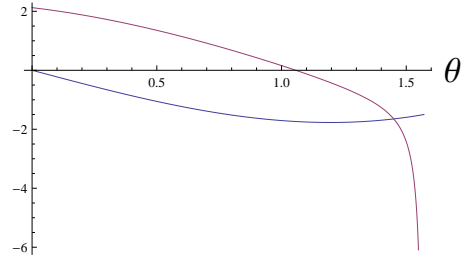


FIG. 12. The two junction conditions for the decompactification geometry. They cross at a negative σ .

As a small bubble in 4D Minkowski space,

$$\bar{A} \frac{\dot{B}_2}{\bar{B}} + \dot{A}_2 = a' = -1. \quad (\text{A8})$$

Combine with Eq. (A3) and (A4), we have

$$\frac{3\bar{B}}{2\bar{A}} \left(\dot{A}_1 + \frac{\bar{A}}{\bar{B}} \dot{B}_1 - 1\right) = \frac{3\sigma}{16\pi\bar{B}m_6^4}. \quad (\text{A9})$$

Note that Eq. (A7) and Eq. (A9) have the same right hand side. Also, since $L = \sqrt{10}m_6^2/\sqrt{\Lambda_6} = 2\sqrt{5}R$, the lefthand sides are just sin and cos. Plotting them between 0 and $\pi/2$, we found that with Eq. (A1) they cross at a positive σ , but with Eq. (A2) they cross at a negative σ . This confirms the argument in Sec.V that Fig.8 violates the null energy condition, and the bubble of nothing geometry in Fig.9 really exists.